TECHNICAL REPORT 74-1

LINEAMENTS IN BASEMENT TERRANE OF THE PENINSULAR RANGES, SOUTHERN CALIFORNIA

by

P. M. Merifield and D. L. Lamar
California Earth Science Corporation
1318 Second Street, Suite 27
Santa Monica, California 90401
Telephone: (213) 395-4528

for

John Tremor, Technical Monitor, NASA-Ames Research Center, Moffett Field, CA 94035

and

Ernest H. Lathram, Technical Officer
U.S. Geological Survey, Menlo Park, CA 94035

Sponsored by NASA-Ames Research Center Contract NAS 2-7698
and U.S. Geological Survey Contract No. 14-08-0001-13911

TECHNICAL REPORT 74-1

LINEAMENTS IN BASEMENT TERRANE OF THE PENINSULAR RANGES, SOUTHERN CALIFORNIA

by

P. M. Merifield and D. L. Lamar
California Earth Science Corporation
1318 Second Street, Suite 27
Santa Monica, California 90401
Telephone: (213) 395-4528

for

John Tremor, Technical Monitor, NASA-Ames
Research Center, Moffett Field, CA 94035

and

Ernest H. Lathram, Technical Officer
U.S. Geological Survey, Menlo Park, CA 94035

Sponsored by NASA-Ames Research Center Contract NAS 207698
and U.S. Geological Survey Contract No. 14-08-0001-13911

PREFACE

Lineaments in the Peninsular Ranges of Southern California are being studied as a portion of broader investigations to apply Skylab and ERTS images to the analysis of fault tectonics and earthquake hazards of Southern California. These investigations are sponsored by NASA-Ames Research Center and the U.S. Geological Survey EROS office. This paper was presented at the First International Conference on the New Basement Tectonics, Salt Lake City, Utah, June 1974, and is to be published in the Proceedings Volume.

ABSTRACT

ERTS and Skylab images reveal a number of prominent lineaments in the basement terrane of the Peninsular Ranges, Southern California. The major, well-known, active, northwest trending, right-slip faults are well displayed; northeast and west to west-northwest trending lineaments are also present. Study of large-scale airphotos followed by field investigations have shown that several of these lineaments represent previously unmapped faults. Pitches of striations on shear surfaces of the northeast and west trending faults indicate oblique-slip movement; data are insufficient to determine the net-slip. These faults are restricted to the pre-Tertiary basement terrane and are truncated by the major northwest trending faults. They may have formed in response to an earlier stress system. All lineaments observed in the space photography are not due to faulting, and additional detailed geologic investigations are required to determine the nature of the unstudied lineaments, and the history and net-slip of fault-controlled lineaments.

INTRODUCTION

The Peninsular Ranges of Southern California extend from the edge of the continental borderland to the Salton Trough and from the Transverse Ranges to the tip of Baja California. In southwestern California, the interior mainland of the Peninsular Ranges province is composed principally of Late Mesozoic plutonic rocks, which comprise the Southern California batholith, and associated roof pendants of metamorphosed Paleozoic and Mesozoic rocks (Jahns, 1954). The structure of the Peninsular Ranges is dominated by northwest trending faults, including the San Jacinto, Whittier-Elsinore, and San Clemente faults (Fig. 1). Additional northwest trending faults in the continental borderland have recently been proposed by Howell et al (1974).

Detailed mapping of central San Clemente Island (Merifield, Lamar, and Stout, 1971) revealed that the structure of the island, which is underlain primarily by Miocene volcanics, is characterized by northeast trending faults and joints. Excellent exposures in the northeast trending, fault-controlled canyons enabled detailed examinations of the fault zones. The faults are predominantly vertical and the pitches (angle in the fault plane measured from the horizontal) of striations on slickensided gouge zones suggest that the principal movement has been oblique, with a major horizontal component. Displacements on the order of tens of meters were observed on a few faults.

Lowman (1969) pointed out that unmapped northeast trending lineaments, expressed primarily by persistent valleys, are prominent on Gemini and Apollo photographs of southwestern California. These lineaments are also obvious on ERTS images (Fig. 2), and their similarity to the northeast trending, fault-controlled canyons on San Clemente Island prompted our investigation of their characteristics. In addition to the northeast trending lineaments described by Lowman, a number of east-west and north-south lineaments are seen in ERTS and Skylab imagery. Aided by large-scale aerial photography, we are conducting field investigations of the most prominent lineaments, to determine their tectonic significance.

Fig. 3 is a sketch map of the most prominent lineaments seen in our study of ERTS and Skylab imagery. The north-south lineament labeled the Chariot Canyon fault has been studied by Allison (1974), who described a

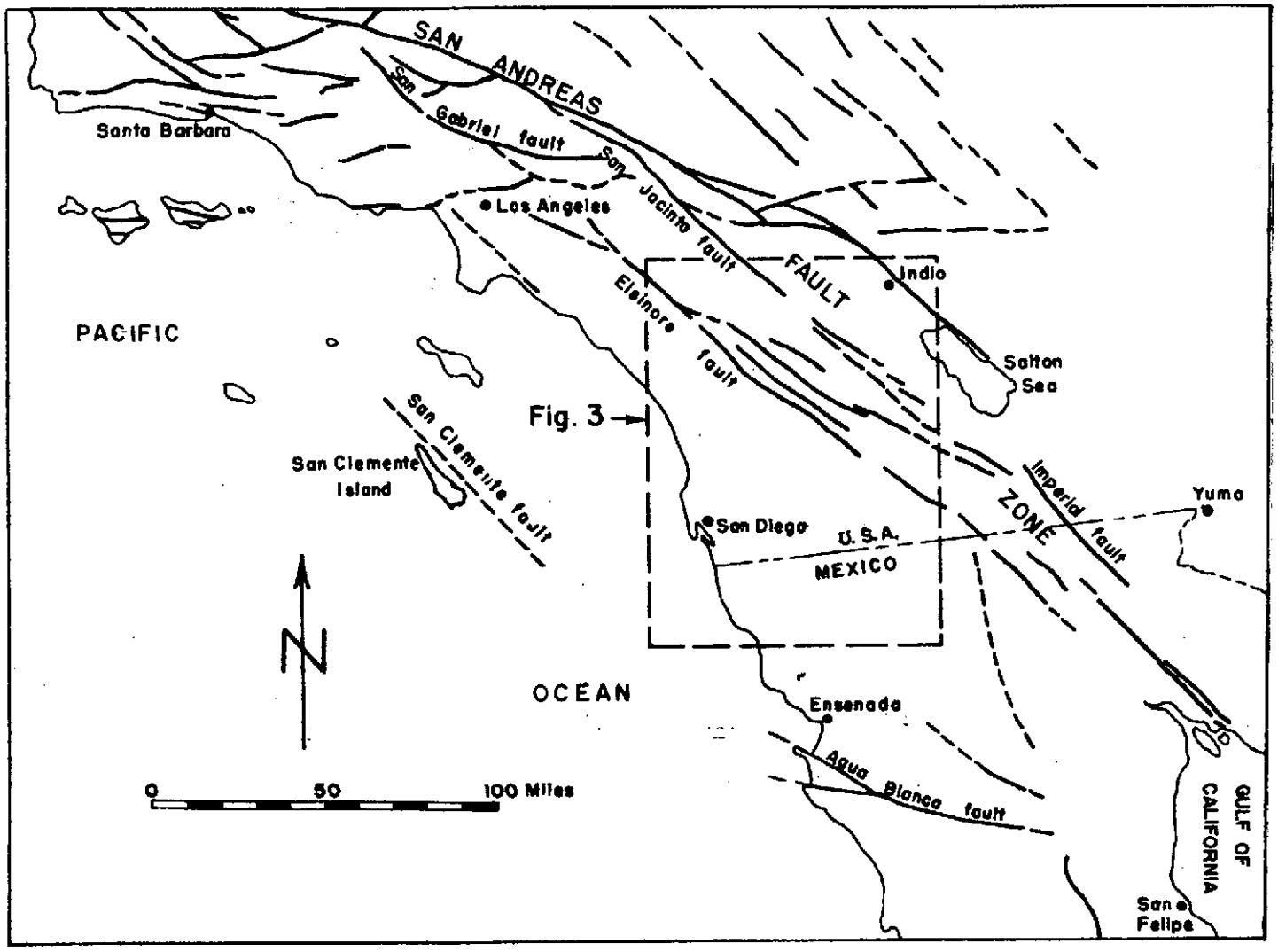

Fig. 1 - Index map showing major northwest-trending faults and area covered by fault and lineament map (Fig. 3). Redrawn from Allen et al (1960).

Fig. 2 - Western half ERTS image 1106-17504, November 6, 1972, Band 7. See Fig. 3 for area covered.

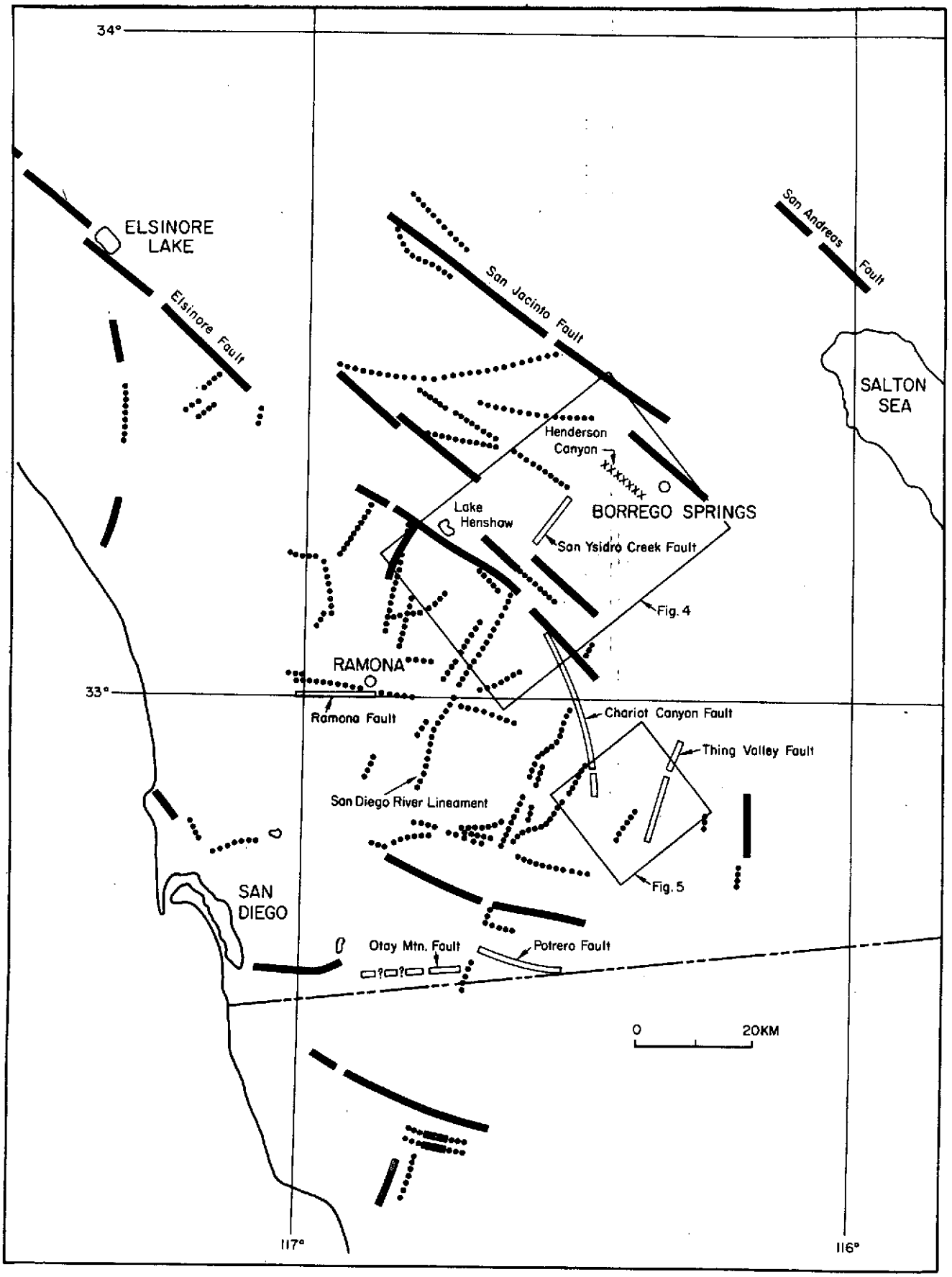

Fig. 3 - Prominent lineaments visible on ERTS and Skylab imagery of southwestern California. Solid lines: faults shown on Strand (1962), Rogers (1965) and Gastil et al (1971). (Faults and lineaments in Mexico appear on ERTS image 1125-17563, November 25, 1972.) Open lines: Previously unmapped faults. Dotted lines: Lineaments of unknown character. XXXXX: Lineament not due to faulting.

fault with a probable right-slip of 8 km. To date, five other lineaments have been identified as faults as a result of our field investigations. One or more of the following criteria were used: 1) a well-developed cataclastic (breccia) zone; 2) slickensided shear surfaces or clay gouge zones, with the attitude of the shear surfaces or gouge zones parallel to the lineament; 3) displaced or terminated lithologic contacts and structures.

Observation of all the characteristics of the lineaments in southwestern California is hampered by the dense growth of chaparral which denies access to large areas. Moreover, zones of mixed rocks or gradational contacts are not easily proven to be displaced. Only in rare cases where abrupt contacts cross at a relatively high angle to the lineament, or in the rarer case where a well-developed fault zone is exposed, can the presence or absence of a fault be determined. Persistent dikes are particularly useful in this regard but unfortunately are restricted in occurrence. Consequently, it is not surprising that the faults discovered in our investigation are not shown on existing maps (which are of a reconnaissance nature, 1:62,500 or smaller scale, and in many cases did not have the benefit of aerial photography). The mapping and compilations of Merriam (1955, 1958), Larson (1948), Rogers (1965), Strand (1962), Gastil et al (1971), Weber (1963), and Jennings (1973) have been invaluable to our studies. However, we have also had the advantage of recently acquired small-scale imagery from ERTS and Skylab spacecraft and high altitude RB-57 aircraft (1:130,000 scale). The perspective afforded by this imagery has focused attention on persistent lineaments, many of which are not obvious in larger-scale photography or on the ground. Although most of the displacements we have observed are not significant at the scale of the previous mapping.

Not all lineaments interpreted from small-scale photography are due to faulting. Therefore, detailed field investigations are required to distinguish those due to faulting from those due to erosion along other planes of weakness such as joints, foliation, and unfaulted contacts, as well as the apparent alignment of quasi-linear features. For example, Henderson Canyon northwest of Borrego Springs appears as a prominent lineament on ERTS (Fig. 2) and Skylab (Fig. 4) images. A field investigation of this feature provided no evidence of faulting. Foliation in banded gneiss along the central segment of Henderson Canyon trends northwest, parallel to the canyon axis; thus,

Fig. 4 - Portion of Skylab 3, Frame 85-374, 190B camera image between Lake Henshaw and Borrego Springs. See Fig. 3 for area covered. Abbreviations: B.S.: Borrego Springs; B.V.C.: Buena Vista Creek; E.F.: Elsinore fault; H.C.: Henderson Canyon; L.H.: Lake Henshaw; S.D.R.: San Diego River; S.Y.C.F.: San Ysidro Creek fault.

Henderson Canyon formed as a result of erosion parallel to the foliation direction.

Field investigations were accomplished to determine the nature and extent of other lineaments noted on ERTS and Skylab images, and descriptions of the individual areas are presented in the following sections. Emphasis is placed on the geologic structure and petrologic descriptions are limited to rocks in and adjacent to the lineaments. More complete descriptions of individual rock units may be found in the references.

THING VALLEY FAULT

Thing Valley and several straight segments of stream canyons to the northeast appear as a prominent north-northeast trending, 20 kilometer-long lineament on ERTS and Skylab images of southeastern San Diego County (Figs. 2 and 5). A conventional air photo and field study was pursued to determine the nature and extent of this feature, and a geologic map (Fig. 6) is the result of that investigation. The distribution of rock units has been modified from an unpublished map prepared by Dr. Richard Merriam (1955). The oldest rock unit is the Julian Schist of probable Triassic age, which consists of quartzite, gneiss, and quartz-mica schist. Mixed rocks consisting of schist and gneissoid quartz diorite of Mesozoic age are also present. These metamorphic and mixed rocks are intruded by the Lakeview Mountain and Green Valley tonalites of Cretaceous age.

Letter symbols on Fig. 6 are keyed to descriptions of individual fault segments. The Elsinore fault and other west-northwest to northwest trending faults in the area between A and B were mapped by Merriam (1955). Bedrock in the area to the south consists of Lakeview Mountain Tonalite, which crops out as scattered light-gray weathering residual blocks. Faults in Lakeview Mountain Tonalite appear on large-scale air photos as straight canyon segments, aligned saddles, linear depressions, and lines of denser vegetation. Over most of their length, the fault zones are covered by boulders; these have apparently accumulated in the low areas eroded in brecciated rock along the fault zone.

A 300-meter-long zone of breccia and fault gouge with grooved and slickensided shear surfaces is exposed at point C. The zone is approximately

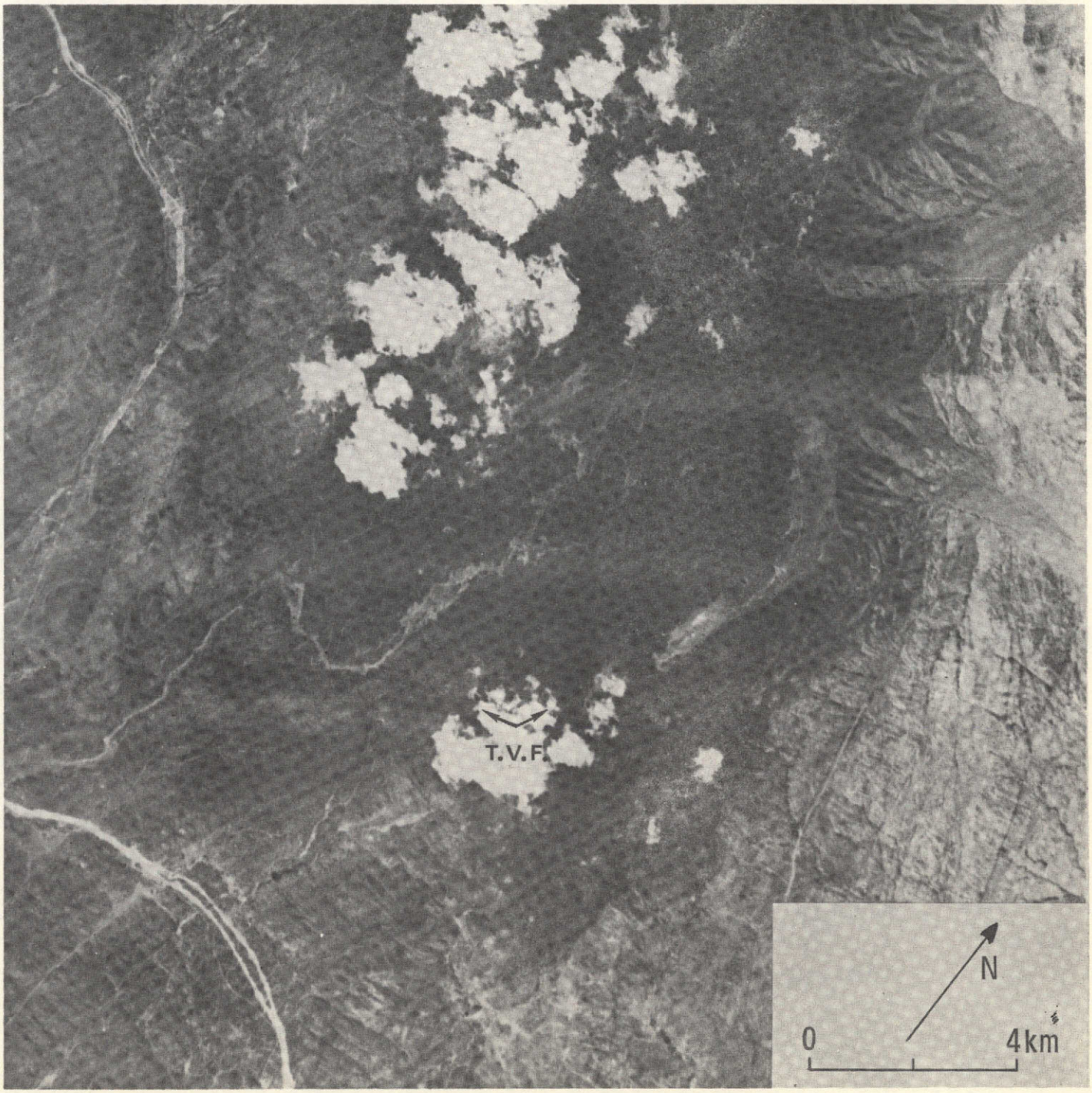

Fig. 5 - Portion of Skylab 3, Frame 85-374, 190B camera image of Thing Valley and vicinity. See Fig. 3 for area covered. T.V.F.: Thing Valley fault.

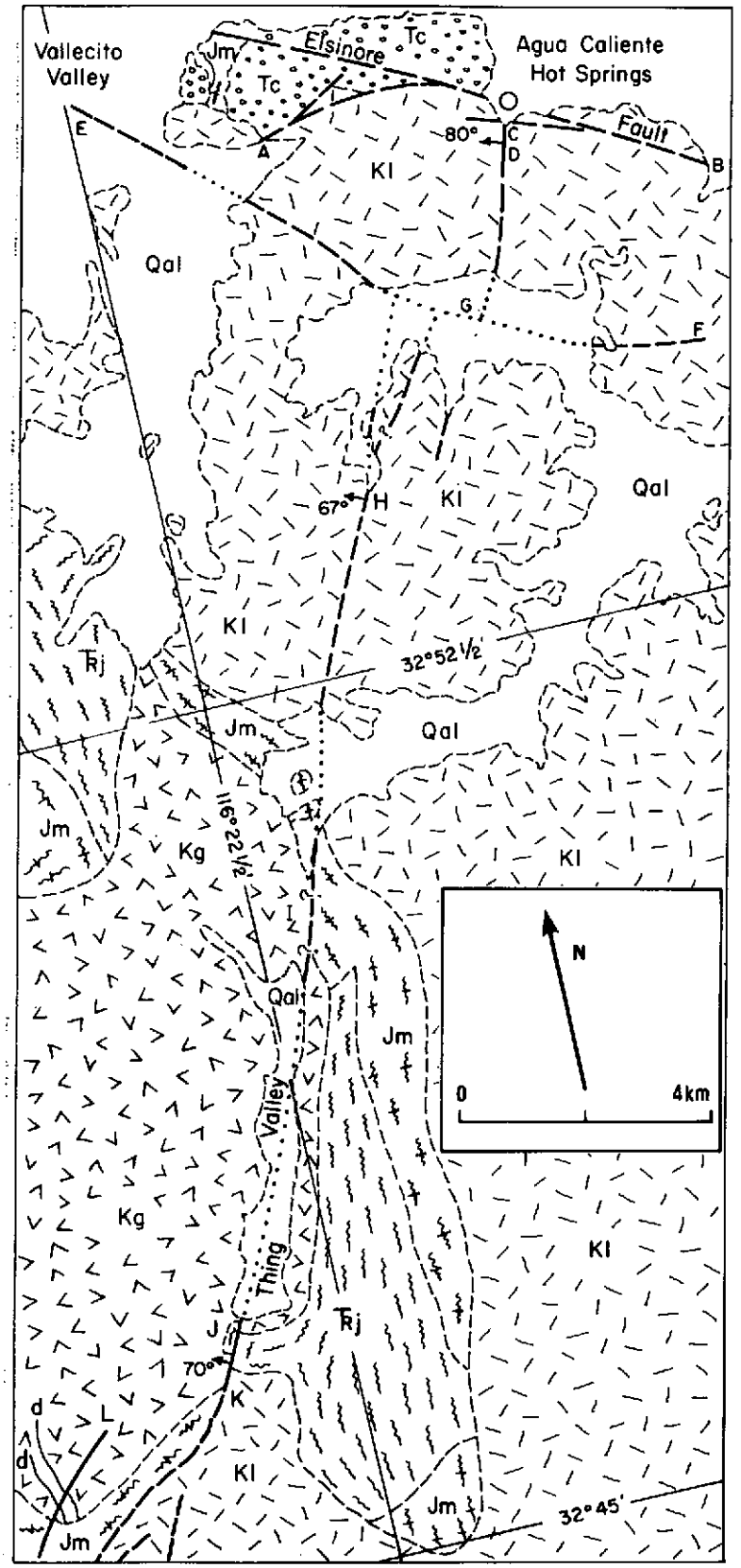

Fig. 6 - Geologic map of Thing Valley area. Geology modified from Merriam (1955) and Buttram (1962); northeast trending faults mapped by authors. Qal: Alluvium, Holocene; Tc: Canebrake Conglomerate, Pliocene non-marine; Kl: Lakeview Mtn. Tonalite, Cretaceous; Kg: Green Valley Tonalite, Cretaceous; Jm: mixed rocks, Jurassic (?); Trj: Julian Schist, Triassic.

7 meters wide at the south end of the exposed fault segment and widens to 35 meters at the northeast end. The relationship with the Elsinore fault to the north is obscured by spring deposits and alluvium in the area of Agua Caliente Springs. A fault zone is exposed 200 meters to the southwest at point D; at this location shear surfaces spaced 2 to 30 cm occur in a 3-meter-wide, 30-meter-long zone of unbroken tonalite. The following attitudes of shear surfaces and pitches of striations were measured at points C and D:

	Strike	Dip	Pitch
C	N2°E	87°E	52°S, 83°S
	N3°E	68°W	none
	N18°E	78°W	47°S
D	N20°E	81°W	85°S
Average	N11°E	80°W	67°S

The lineament on large-scale air photos in this area has a trend of N15°E.

The location of the northwest to east-west trending fault between points E and F has been modified from previous mapping by Merriam (1955) and Buttram (1962). A search for breccia and gouge along the trace observed on air photos was not accomplished during the present investigation. This fault is inferred to continue west to join the Elsinore fault (Merriam, 1955). In Vallecito Valley, the fault is reflected as a line of vegetation apparently caused by ground water blockage upstream of the fault, and Buttram (1962) has reported a fault scarp in alluvium at this location. At point G, traces of the Thing Valley fault appear to have 700 to 1300 meters of right separation along this branch of the Elsinore fault. It is impossible to prove that any of the faults between H and D were ever continuous; however, previous alignment is suggested by similar attitudes of the fault segments and fault slip is in the expected sense.

A 25-meter-wide zone of light-gray breccia and red-brown fault gouge is exposed in two east-west trending gullies at point H (Fig. 7). Slickensided shear surfaces in the fault zone strike between N32°E and N54°E and dip 59°to 78° to the northwest; the representative dip is 67°. The lineament observed on air photos in this area strikes approximately N24°E. No

Fig. 7 - Exposure of fault gouge within a brecciated zone at point H, Fig. 6. View to north, hammer at left margin for scale.

grooves or striations were observed on slickensided surfaces parallel to the fault zone.

A straight, deep canyon aligned with the fault zone is present at I. Thing Valley to the south-southwest is a narrow, straight feature along the same alignment (Fig. 5). We infer that Thing Valley and canyon I developed as a result of erosion of fault gouge and breccia within the fault zone. Alluvium within Thing Valley, alluvium, talus, and dense brush at canyon I obscure the geologic relations, and the existence of a fault zone cannot be proven. Field mapping and the study of large-scale air photos suggest as much as 1 km of right separation of the zone of mixed rock along canyon I. However, the steeply dipping foliation trends in these rocks vary from N36°E to N26°W; consequently, the apparent displacement could be explained by curving contacts.

Southwest of Thing Valley, exposures are much poorer than in the desert northeast of Thing Valley. However, the fault is exposed in a roadcut crossing a north-northeast trending saddle (J on Fig. 6) where the fault separates schist on the east from Green Valley Tonalite on the west. Twelve meters of brecciated schist lie east of an 8-10 cm gouge zone with a strike of N30°-35°E and a dip of 70°W. The breccia zone west of the gouge may be as much as 18 m wide, but the zone is largely covered by colluvium. The northwest trending contact between schist and intrusive rocks has a right separation of about 100 m; the dip of the contact is not known. Southwest of the roadcut the relations are obscure owing to dense brush, but air photos suggest the fault splays out into several branches, one of which (at K on Fig. 6) is shown on Merriam's (1955) map.

Another fault to the west (L on Fig. 6) follows a northeast trending valley parallel to the faults discussed above. A left separation of 73 m is clearly evidenced by offset granite pegmatite dikes; the attitude of the dikes is N13°W, 42°W. Insufficient data are available to determine the sense of slip along this fault.

We conclude that the Thing Valley lineament is the expression of a fault over 20 km in length. Pitches of striations within the fault zone suggest oblique movement with the west block moving upward and northeastward relative to the east block (reverse right-slip fault). Possible

right-slip varies from 100 m near the southwest end to as much as 1 km along the central portion of the fault.

SAN YSIDRO CREEK FAULT

A segment of San Ysidro Creek and a stream canyon to the south form a prominent 7-km-long north-northeast trending lineament on space imagery (Figs. 2 and 4). The San Diego River Valley southwest of the Elsinore fault zone forms a similar, prominent, 30-km-long lineament 10 km to the south-southwest; these two features are approximately aligned, but Skylab and ERTS images as well as larger scale air photos clearly show that the San Ysidro and San Diego Valley lineaments are not continuous.

Figure 8 is a geologic map of the San Ysidro Creek area. South of latitude 33°15', the area was mapped by Merriam (1958) and Scheliga (1963), and the entire area is shown on small-scale maps prepared by Weber (1963) and Rogers (1965). The northwest portion of the area is underlain by Lakeview Mountain Tonalite, which is characterized by prominent, near-vertical east-west jointing. Julian Schist exposed to the southeast consists of biotite schist interlayered with gneiss and hornfels. Foliation in the metamorphic rocks generally trends north-northeast, parallel to the intrusive contact and the San Ysidro Creek lineament. Locally, however, the foliation is undulatory and not parallel to the lineament.

The steep slopes and dense brush limit access to areas underlain by bedrock. Alluvium in the stream valleys, as well as terrace deposits and thick soil in the southern portion of the area, further obscure the underlying structure. The faults shown on Fig. 8 appear as distinct lineaments on large-scale air photos, but the fault zone is exposed only in roadcuts at the location of the dip symbol. A zone of crushed and sheared gouge up to 7 meters wide, with striations on shear surfaces, is present. The following attitudes and pitches of striations on shear surfaces were noted:

	Strike	Dip	Pitch
	N3°W	85°W	1°S
	N4°W	62°E	3°S
	N50°E	90°	7°S
	N5°W	74°E	20°S
	N26°E	74°E	none
Average	N13°E	79°E	8°S

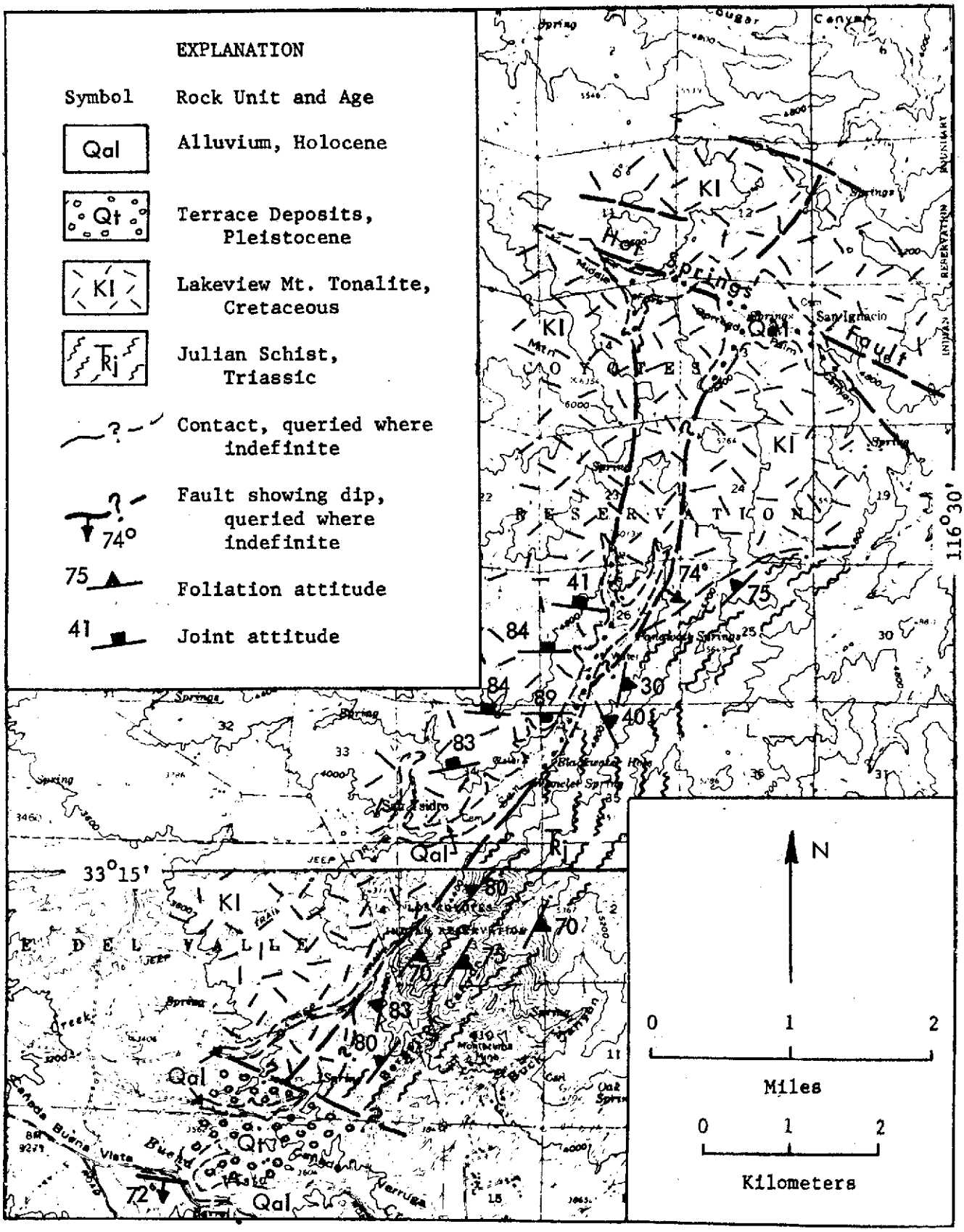

Fig. 8 – Geologic map of the San Ysidro Creek area. Hot Spring fault from Weber (1963); fault truncating south end of San Ysidro Creek fault from Merriam (1958) and Scheliga (1963).

The average value of N13°E lies between the N8°E trend of the lineaments branching to the north and the N37°E trend of the principal lineament to the southwest. It is inferred from this exposure that the lineaments extending to the northeast and southwest on the air photos are faults. The striations on shear surfaces suggest predominately horizontal movement. No data are available to determine the amount and sense of displacement.

In the northern portion of the area, the postulated fault splits into two branches which can be traced through massive tonalite to the Middle Fork of Borrego Palm Canyon. From our analysis of the air photos, we conclude that the San Ysidro fault abuts the northwest trending Hot Springs fault in the Middle Fork of Borrego Palm Canyon shown by Weber (1963) and Rogers (1965).

Over most of its postulated trace to the south, the fault parallels the average foliation in metamorphic rock and may coincide with the intrusive contact. South of the roadcut fault exposure, a prominent line of denser vegetation can be traced for 1 km along the southeast side of San Ysidro Valley. Additional alignments of straight canyon segments and intervening saddles to the south are believed to be a further extension of the San Ysidro Creek fault.

Structural relations near the south end of the San Ysidro Creek fault are obscured by thick brush and soil. The fault contact between basement rock and terrace deposits is based on mapping by Merriam (1958) and Scheliga (1963). Exposures within the limited area studied in the present investigation are not sufficient to verify the existence of this segment of the fault. One kilometer farther southwest, Weber (1963) shows a northwest trending fault along the course of Buena Vista Creek. A fault zone with an attitude of N83°W, 72°S is exposed in the roadcut directly southwest of the San Ysidro fault along the south side of Buena Vista Creek, and this may be a branch of the fault mapped by Weber (1963). Our study of large-scale air photos reveals no evidence of a northeast trending fault south of Buena Vista Creek and we conclude that the south end of the San Ysidro fault is truncated by a northwest trending fault.

OTHER FAULTS

The Potrero fault is exposed in roadcuts along the north side of

Highway 94, 4.8 km east of Potrero, as a zone of breccia, gouge, and slickensided shear surfaces (Fig. 9). The zone is up to 4 meters wide, trends N70°W, and dips 80°S; pitches of 75°E and 10°E were measured on striations on shear surfaces in the fault zone. The fault appears on RB-57 photos as a prominent lineament over 11 km long.

The Otay Mountain fault trends nearly east-west along the north flank of Otay Mountain, 2.5 km north of the Mexican border. It was first recognized as a prominent lineament on ERTS and RB-57 photographs. The eastern part of the lineament is a fault with about 120 m left separation of Santiago Peak volcanic flows. The flows dip 40° northeast; insufficient data are available to determine the net-slip. The western extension of the lineament is inferred to be a fault, but no exposures have been observed and individual flows have not been matched across the fault.

The Ramona fault is exposed in a roadcut where a prominent lineament (Warren Canyon) crosses Highway 67, 8 km southwest of Ramona. A 3-meter-wide, gray clay gouge zone is present about midway in a zone of breccia and shear surfaces at least 30 m wide. Striations on shear surfaces are vertical. The fault is entirely in granodiorite, and hence the displacement is unknown.

Most of the remaining lineaments (dotted on Fig. 3) have either not been investigated in sufficient detail in the field to determine their characteristics, or no conclusive evidence of faulting could be found.

REGIONAL TRENDS OF FAULTS AND LINEAMENTS

Roadcuts in basement rock throughout this portion of the Peninsular Ranges were examined to determine the attitude of fault zones and the pitch of striations on slickensided shear surfaces. The exposures were selected for their well-developed fault zones rather than for any relation to lineaments on the ERTS and Skylab images. These observations were combined with measurements on the specifically studied individual faults and are summarized on Fig. 10. The observations were made to determine if there is any relationship between the directions of individual fault zones and the lineament trends (Fig. 11). With the exception of the northeast trend, no close relationships are apparent.

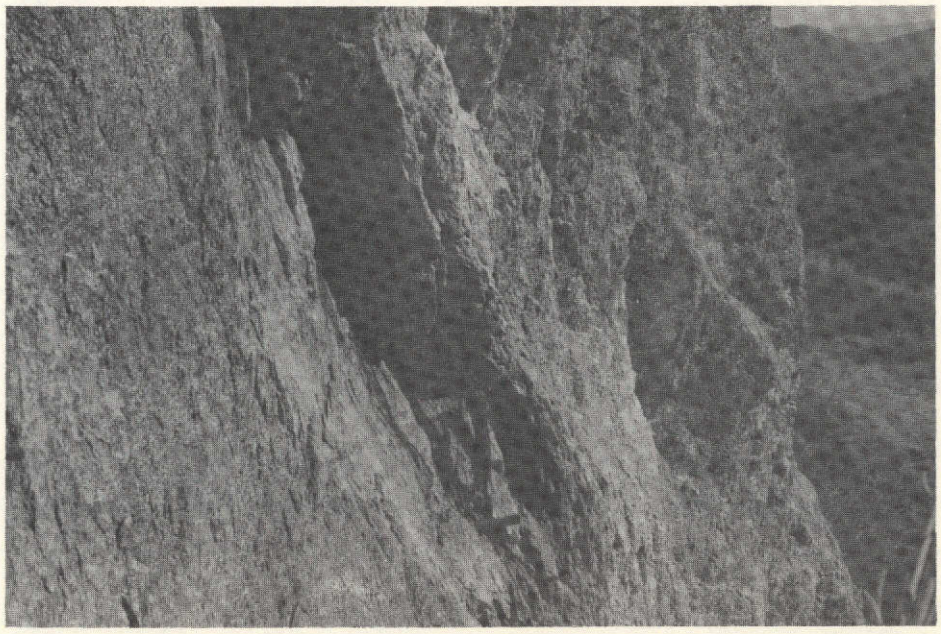

Fig. 9 - Exposure of Potrero fault in roadcut on the north side of Highway 94, 4.8 km east of Potrero, showing slickensided shear surfaces.

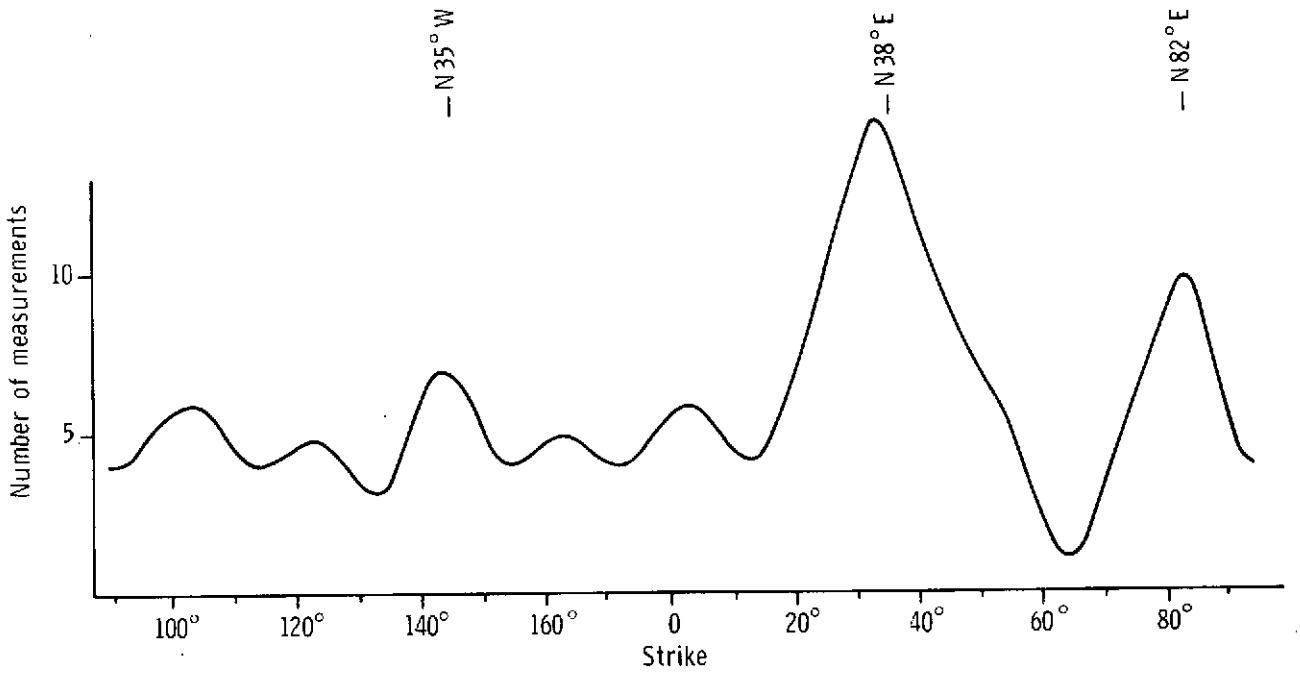

Fig. 10 - Shear zones, Peninsular Ranges of Southern California, 109 strikes, 10° intervals.

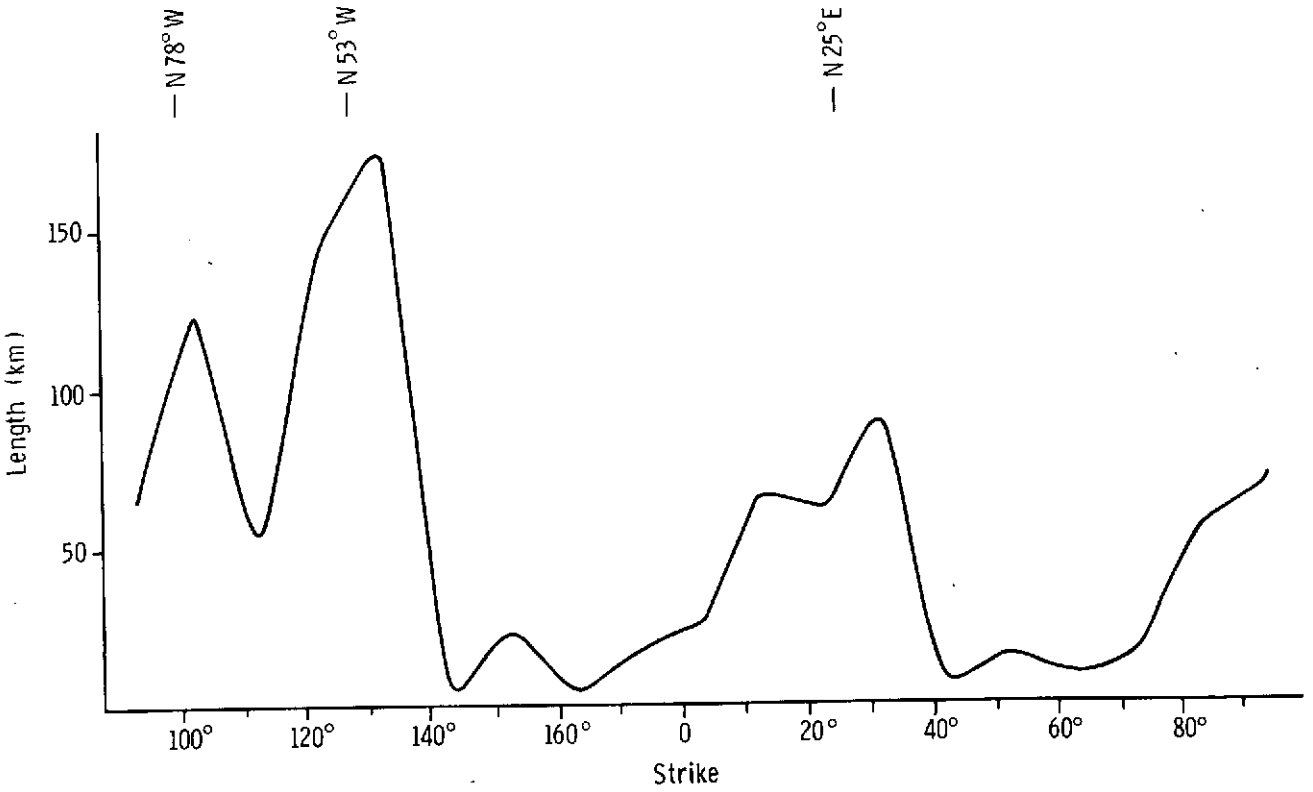

Fig. 11 - Lineaments shown in Fig. 3, length vs. strike, 10° intervals.

CONCLUSIONS AND DISCUSSION

Our conclusions are as follows:

1. Small-scale photography from ERTS, Skylab, and high-altitude aircraft have revealed several prominent lineaments in the basement terrane of southwestern California. Field investigations have shown that some of these lineaments are previously unrecognized faults, up to 24 km in length.

2. Three principal fault and lineament sets were observed: northwest, northeast, and west to west-northwest.

3. The northwest faults show the latest movement; they are nowhere cut by faults in the other sets.

4. The northeast and west trending faults we have studied have relatively small displacement, ranging from tens of meters to perhaps 1 km. In contrast, a large amount of right-slip has been reported on the major northwest trending faults; for example, 24 km on San Jacinto (Sharp, 1967) and 30 to 40 km on the Elsinore fault (Lamar, 1961; Sage, 1973).

5. The northeast and west trending faults are steeply dipping and display well-developed breccia zones and slickensided shear surfaces. Pitches of striations on shear surfaces suggest oblique movement. Data are usually insufficient to determine sense of slip and net-slip. None of the faults that we have investigated have been found to cut post-Mesozoic sediments.

Data are insufficient to draw conclusions about the tectonic significance of the faults described in this paper. One possibility is that the northwest and northeast trending faults form a conjugate shear system; however, this would require that the northeast trending faults are left-slip, but this has not been demonstrated. On the contrary, a right-slip component is probable on the Thing Valley fault. Another possibility is that the northeast and west trending faults are conjugate shears related to a stress system older than the present one with east-northeast, west-southwest crustal shortening. In this case, the west trending faults would be left-slip.

Future work should be directed toward determining whether the northeast and west trending faults are related to the presently active stress

system or to an older inactive system, partly because this question relates to the earthquake risk in the vicinity of these faults. Additional detailed geologic investigations are required to establish which of the other lineaments are faults and to determine the age, sense, and amount of movement on them.

ACKNOWLEDGMENTS

The work reported herein was accomplished under NASA Contract NAS 2-7698 and U.S. Geological Survey Contract 14-08-0001-13911. We wish to acknowledge valuable discussions with Richard Merriam and Mason Hill; Richard Merriam kindly loaned us his unpublished field maps of the Thing Valley area, and Mason Hill critically read the manuscript. Thomas W. Troutman, a student at the University of California, Los Angeles assisted in the geologic mapping of the San Ysidro Creek area.

REFERENCES

Allen, C.R., Silver, L.T., and Stehle, F.G., 1960, Agua Blanca fault - a major transverse structure of northern Baja California, Mexico: Geol. Soc. Am., Bull., vol. 71, p. 457-482.

Allison, L., 1974, Tectonic relationship of the Elsinore fault zone and the Chariot Canyon fault, San Diego County, California: Abstracts with program, Geol. Soc. Amer., Cordilleran Section, p. 138.

Buttram, G.N., 1962, The geology of the Agua Caliente Quadrangle, California: Unpublished Master's thesis, Univ. of Southern Calif.

Gastil, R.G., Phillips, R.P., and Allison, E.C., 1971, Reconnaissance Geologic Map of the State of Baja California: Geol. Soc. America, Scale: 1:250,000.

Howell, D.G., Stuart, C.J., Platt, J.P. and Hill, D.J., 1974, Possible strike-slip faulting in the southern California borderland: Geology, v. 2, No. 2, p. 101-104.

Jahns, R.H., 1954, Geology of the Peninsular Ranges Province, Southern California and Baja California: in Calif. Div. Mines and Geol., Bull. 170, Ch. 2, p. 29-52.

Jennings, C.W., 1973, State of California, preliminary fault and geologic map, scale 1:750,000: Calif. Div. Mines and Geol., Preliminary Report 13.

Lamar, D.L., 1961, Structural evolution of the northern margin of the Los Angeles basin: Ph.D. thesis, U.C.L.A. p. 142.

Larsen, E.S., Jr., 1948, Batholith and Associated Rocks of Corona, Elsinore, and San Luis Rey Quadrangles, Southern California: Geol. Soc. Amer. Memoir 29.

Lowman, P.D., 1969, Apollo 9 multispectral photography: geologic analysis: NASA Goddard Space Flight Center, Greenbelt, Md., X-644-69-423.

Merifield, P.M., Lamar, D.L., and Stout, M.L., 1971, Geology of central San Clemente Island, California: Geol. Soc. Am., Bull., vol. 82, p. 1989-1994.

Merriam, R., 1955, Geologic map of Cuyapaipe Quadrangle, California, scale 1/62,500: unpublished map (Cuyapaipe Quad. presently designated Mt. Laguna Quad).

Merriam, R., 1958, Geology and mineral resources of Santa Ysabel quadrangle, San Diego County, California: Calif. Div. Mines, Bull. 177, p. 42.

Rogers, T.H., 1965, Geologic map of California, Santa Ana Sheet: Calif. Div. of Mines and Geology.

Sage, O.G., Jr., 1973, Paleocene geography of the Los Angeles region: in proc. of the Conf. on Tectonic problems of the San Andreas Fault System, Stanford Univ. Publ., Geol. Sci., v. XIII, p. 348-357.

Scheliga, J.T., Jr., 1963, Geology and water resources of Warner Basin, San Diego County, California: unpublished Master's thesis, Univ. of Southern Calif.

Sharp, R.V., 1967, San Jacinto fault zone in the Peninsular Ranges of southern California: Geol. Soc. Am., Bull, v. 78, p. 705-730.

Strand, R.G., 1962, Geologic map of California, San Diego-El Centro Sheet: Calif. Div. of Mines and Geology.

Weber, F.H., 1963, Geology and mineral resources of San Diego County, California: Calif. Div. Mines and Geology, county report 3, 309 p.